J|A|C|S ARTICLES

Published on Web 09/08/2009

Probing Flexibility in Porphyrin-Based Molecular Wires Using Double Electron Electron Resonance

Janet E. Lovett,*,†,‡ Markus Hoffmann,§ Arjen Cnossen,§ Alexander T. J. Shutter,§ Hannah J. Hogben,§ John E. Warren,⊥ Sofia I. Pascu,|| Christopher W. M. Kay,# Christiane R. Timmel,†,§ and Harry L. Anderson*,§

Centre for Advanced Electron Spin Resonance, Inorganic Chemistry Laboratory, University of Oxford, South Parks Road, Oxford OX1 3QR, United Kingdom, Sir William Dunn School of Pathology, University of Oxford, South Parks Road, Oxford OX1 3RE, United Kingdom, Deptartment of Chemistry, Chemistry Research Laboratory, University of Oxford, Mansfield Road, Oxford, OX1 3TA, United Kingdom, Synchrotron Radiation Source, Daresbury Laboratory, Warrington WA4 4AD, United Kingdom, Department of Chemistry, University of Bath, Bath BA2 7AY, United Kingdom, and Institute of Structural and Molecular Biology and London Centre for Nanotechnology, University College London, Gower Street, London WC1E 6BT, United Kingdom

Received July 13, 2009; E-mail: janet.lovett@path.ox.ac.uk; harry.anderson@chem.ox.ac.uk

Abstract: A series of butadiyne-linked zinc porphyrin oligomers, with one, two, three, and four porphyrin units and lengths of up to 75 Å, have been spin-labeled at both ends with stable nitroxide TEMPO radicals. The pulsed EPR technique of double electron electron resonance (DEER) was used to probe the distribution of intramolecular end-to-end distances, under a range of conditions. DEER measurements were carried out at 50 K in two types of dilute solution glasses: deutero-toluene (with 10% deutero-pyridine) and deutero-*o*-terphenyl (with 5% 4-benzyl pyridine). The complexes of the porphyrin oligomers with monodentate ligands (pyridine or 4-benzyl pyridine) principally adopt linear conformations. Nonlinear conformations are less populated in the lower glass-transition temperature solvent. When the oligomers bind star-shaped multidentate ligands, they are forced to bend into nonlinear geometries, and the experimental end-to-end distances for these complexes match those from molecular mechanics calculations. Our results show that porphyrin-based molecular wires are shape-persistent, and yet that their shapes can deformed by binding to multivalent ligands. Self-assembled ladder-shaped 2:2 complexes were also investigated to illustrate the scope of DEER measurements for providing structural information on synthetic noncovalent nanostructures.

Introduction

Long π-conjugated oligomers, or molecular wires, are widely investigated because of their ability to mediate electron transfer,[1] and because of their strong nonlinear optical behavior.[2,3] To understand the structure−property relationships governing these molecules, we need information on their three-dimensional shapes. It is often assumed that molecular wires are rigid units, but as they become longer they inevitably become more flexible. Despite recent advances in small-angle neutron scattering[4] and X-ray scattering[5] techniques, it remains difficult to probe the conformations of molecules in solution on the 2 to 10 nm length-scale. Förster resonance energy transfer (FRET) is widely used to monitor the conformations of biopolymers on this length-scale, after attachment of suitable donor and acceptor chromophores.[6] However, it would be difficult to use FRET to measure the distance between two points on a molecular wire because the π-system of the wire would participate in the energy transfer process and differential labeling is typically required. Double electron electron resonance (DEER) is a pulsed EPR technique for measuring distances between paramagnetic centers, using dipole−dipole coupling.[7−11] If the distance, R, between two localized organic radical centers is more than about 1.5

† Centre for Advanced Electron Spin Resonance, University of Oxford.
‡ Sir William Dunn School of Pathology, University of Oxford.
§ Department of Chemistry, University of Oxford.
⊥ Daresbury Laboratory.
|| University of Bath.
University College London.

(1) Tao, N. J. *Nat. Nanotechnol.* **2006**, *1*, 173–181.
(2) Tykwinski, R. R.; Gubler, U.; Martin, R. E.; Diederich, F.; Bosshard, C.; Gunter, P. *J. Phys. Chem. B* **1998**, *102*, 4451–4465.
(3) Pawlicki, M.; Collins, H. A.; Denning, R. G.; Anderson, H. L. *Angew. Chem., Int. Ed.* **2009**, *48*, 3244–3266.
(4) Lei, S.; Ver Heyen, A.; De Feyter, S.; Surin, M.; Lazzaroni, R.; Rosenfeldt, S.; Ballauff, M.; Lindner, P.; Mössinger, D.; Höger, S. *Chem.—Eur. J.* **2009**, *15*, 2518–2535.
(5) Easwaramoorthi, S.; Jang, S. Y.; Yoon, Z. S.; Lim, J. M.; Lee, C.-W.; Mai, C.-L.; Liu, Y.-C.; Yeh, C.-Y.; Vura-Weis, J.; Wasielewski, M. R.; Kim, D. *J. Phys. Chem. A* **2008**, *112*, 6563–6570.
(6) Hass, E. *ChemPhysChem* **2005**, *6*, 858–870.
(7) Larsen, R. G.; Singel, D. J. *J. Chem. Phys.* **1993**, *98*, 5134–5146.
(8) Milov, A. D.; Maryasov, A. G.; Tsvetkov, Y. D. *Appl. Magn. Reson.* **1998**, *15*, 107–143.
(9) Tsvetkov, Y. D.; Milov, A. D.; Maryasov, A. G. *Russ. Chem. Rev.* **2008**, *77*, 487–520.
(10) Schiemann, O.; Prisner, T. F. *Q. Rev. Biophys.* **2007**, *40*, 1–53.
(11) Jeschke, G.; Polyhach, Y. *Phys. Chem. Chem. Phys.* **2007**, *9*, 1895–1910.

 10.1021/ja905796z CCC: $40.75

nm, then the dipole−dipole coupling energy is inversely proportional to R.[3] The DEER technique measures the coupling frequency by monitoring how a refocused echo, at one microwave frequency, is affected by a 180° microwave pulse at a second frequency. DEER has been widely used to measure distances in the 1.5−7.5 nm range in peptides, proteins, protein complexes, and polynucleotides,[9−17] and it is a promising technique for probing the conformations of molecular wires[18−21] and other rodlike molecules.[22−25]

The high polarizability and electronic delocalization of the porphyrin macrocycle make it an ideal unit from which to construct molecular wires,[26−29] and conjugated porphyrin oligomers exhibit a range of wirelike behavior including long-range charge transport,[30−33] high conductance,[34] rapid exciton migration,[35] and large two-photon absorption cross-sections.[36,37] Supramolecular self-assembly can be used to control the torsional angles in these molecular wires and thus to control their electronic delocalization.[33,37,38] Coordination to multidentate ligands can also be used to bend porphyrin-based molecular wires, as illustrated by the template-directed synthesis of porphyrin nanorings,[39,40] which leads to the question of whether these molecules should be regarded as shape-persistent. Here we report a series of DEER distance measurements on butadiyne-linked porphyrin oligomers terminated with stable TEMPO radicals, **P1**−**P4** (Figure 1). The results show that they are shape-persistent, and yet that their shapes can readily be deformed by binding to ligands such as **L1** and **L2**. Assembly of ladder complexes by binding oligomers **P2** and **P3** with ligand **L3** has also been confirmed by DEER distance measurements. The crystal structure of a bis-TEMPO porphyrin monomer **P1′** (identical to **P1** except with different solubilizing side chains) has been solved and the crystallographic radical−radical distance compares well with the DEER results.

Methods and Materials

Synthesis. Full experimental details for the synthesis and characterization of compounds **P1**−**P4**, **P1′**, **L1** and **L3** are provided in the Supporting Information. The synthesis of **L2** has been reported previously.[39]

UV−Vis−NIR Titrations. The stability constants and stoichiometries of the complexes **P2**·**L1**, **P4**·**L2**, and (**P2**)$_2$·(**L3**)$_2$ were measured by UV−vis−NIR titration in toluene at 298 K. See the Supporting Information for titration spectra and binding isotherms.

X-ray Crystallography. Crystals of the monomer with 3,5-di-*tert*-butylphenyl side chains, **P1′**, were grown by vapor diffusion of methanol into a solution of the porphyrin in dioxane. X-ray diffraction data were collected at the synchrotron at Daresbury UK. See the Supporting Information for further details; CCDC 725782.

Molecular Dynamics (MD) Calculations. Molecular dynamics simulations were performed in HyperChem with a temperature of 180 K without explicit solvent for a simulation period of 500 ps. The X-ray crystal structure of porphyrin monomer **P1′** was used to refine the MM+ force field parameters. More details are given in the Supporting Information.

DEER Experiments. The oligomers without templates were dissolved in d_8-toluene with 10% d_5-pyridine (d_8 -PhMe/Py) and d_{14}-*o*-terphenyl with 5% 4-benzylpyridine (d_{14}-*o*TP/BnPy). The monodentate ligands Py and BnPy were added to coordinate the zinc centers to prevent aggregation. The complexes of **L1**, **L2**, and **L3** were measured in d_8-PhMe.

The four-pulse DEER sequence was performed at X-band (~9.3 GHz) with a Bruker ELEXSYS 680 EPR spectrometer. The tubes with frozen sample were inserted into a 3 mm split ring resonator (Bruker EN 4118X-MS3). The experiments were conducted at 50 K using a $(\pi)/(2)-\tau_1-\pi-(\tau_1 + t)-\pi_{pump}-(\tau_2 - t)-\pi-\tau_2-$echo pulse sequence with 32 ns pulses at the observer frequency and a 12 ns pump frequency pulse. The frequency of the π_{pump} pulse was set to the maximum of the nitroxide echo detected field sweep spectrum and the observer frequency was offset by 65 MHz (see the Supporting Information for exceptions). A ± phase cycle was applied to the first observer pulse to remove receiver offsets. The τ_1 was set at 400 ns for deuterated solvents and was stepped eight times in 56 ns increments to average out deuterium modulations from hyperfine coupling to the solvent matrix. τ_2 ranged between 4.5 and 16 μs. The time, t, was incremented in either 8 or 16 ns steps and hence each time trace normally consisted of between 500

(12) Jeschke, G.; Bender, A.; Paulsen, H.; Zimmermann, H.; Godt, A. *J. Magn. Reson.* **2004**, *169*, 1–12.
(13) Denysenkov, V. P.; Prisner, T. F.; Stubbe, J.; Bennati, M. *Proc. Natl. Acad. Sci.* **2006**, *103*, 13386–13390.
(14) Georgieva, E. R.; Ramlall, T. F.; Borbat, P. P.; Freed, J. H.; Eliezer, D. *J. Am. Chem. Soc.* **2008**, *130*, 12856–12857.
(15) Alexander, N.; Bortolus, M.; Al-Mestarihi, A.; Mchaourab, H.; Meiler, J. *Structure* **2008**, *16*, 181–195.
(16) Kay, C. W. M.; El Mkami, H.; Cammack, R.; Evans, R. W. *J. Am. Chem. Soc.* **2007**, *129*, 4868–4869.
(17) Banham, J. E.; Baker, C. M.; Ceola, S.; Day, I. J.; Grant, G. H.; Groenen, E. J. J.; Rodgers, C. T.; Jeschke, G.; Timmel, C. R. *J. Magn. Reson.* **2008**, *191*, 202–218.
(18) Martin, R. E.; Pannier, M.; Diederich, F.; Gramlich, V.; Hubrich, M.; Spiess, H. W. *Angew. Chem., Int. Ed.* **1998**, *37*, 2834–2837.
(19) Godt, A.; Schulte, M.; Zimmermann, H.; Jeschke, G. *Angew. Chem., Int. Ed.* **2006**, *45*, 7560–7564.
(20) Margraf, D.; Bode, B. E.; Marko, A.; Schiemann, O.; Prisner, T. F. *Mol. Phys.* **2007**, *105*, 2153–2160.
(21) Bode, B. E.; Margraf, D.; Plackmeyer, J.; Dürner, G.; Prisner, T. F.; Schiemann, O. *J. Am. Chem. Soc.* **2007**, *129*, 6736–6745.
(22) Pornsuwan, S.; Bird, G.; Schafmeister, C. E.; Saxena, S. *J. Am. Chem. Soc.* **2006**, *128*, 3876–3877.
(23) Bird, G. H.; Pornsuwan, S.; Saxena, S.; Schafmeister, C. E. *ACS Nano* **2008**, *2*, 1857–1864.
(24) Lovett, J. E.; Bowen, A. M.; Timmel, C. R.; Jones, M. W.; Dilworth, J. R.; Caprotti, D.; Bell, S. G.; Wong, L. L.; Harmer, J. *Phys. Chem. Chem. Phys.* **2009**, *11*, 6840–6848.
(25) Raitsimring, A. M.; Gunanathan, C.; Potapov, A.; Efremenko, I.; Martin, J. M. L.; Milstein, D.; Goldfarb, D. *J. Am. Chem. Soc.* **2007**, *129*, 14138–14139.
(26) Crossley, M. J.; Burn, P. L. *J. Chem. Soc., Chem. Commun.* **1991**, 1569–1571.
(27) Lin, V. S.-Y.; DiMagno, S. G.; Therien, M. J. *Science* **1994**, *264*, 1105–1111.
(28) Anderson, H. L. *Chem. Commun.* **1999**, 2323–2330.
(29) Tsuda, A.; Osuka, A. *Science* **2001**, *293*, 79–82.
(30) Kang, B. K.; Aratani, N.; Lim, J. K.; Kim, D.; Osuka, A.; Yoo, K.-H. *Chem. Phys. Lett.* **2005**, *412*, 303–306.
(31) Susumu, K.; Frail, P. R.; Angiolillo, P. J.; Therien, M. J. *J. Am. Chem. Soc.* **2006**, *128*, 8380–8381.
(32) Winters, M. U.; Dahlstedt, E.; Blades, H. E.; Wilson, C. J.; Frampton, M. J.; Anderson, H. L.; Albinsson, B. *J. Am. Chem. Soc.* **2007**, *129*, 4291–4297.
(33) Grozema, F. C.; Houarner-Rassin, C.; Prins, P.; Siebbeles, L. D. A.; Anderson, H. L. *J. Am. Chem. Soc.* **2007**, *129*, 13370–13371.
(34) Sedghi, G.; Sawada, K.; Esdaile, L. J.; Hoffmann, M.; Anderson, H. L.; Bethell, D.; Haiss, W.; Higgins, S. J.; Nichols, R. J. *J. Am. Chem. Soc.* **2008**, *130*, 8582–8583.
(35) Chang, M.-H.; Hoffmann, M.; Anderson, H. L.; Herz, L. M. *J. Am. Chem. Soc.* **2008**, *130*, 10171–10178.
(36) Drobizhev, M.; Stepanenko, Y.; Dzenis, Y.; Karotki, A.; Rebane, A.; Taylor, P. N.; Anderson, H. L. *J. Phys. Chem. B.* **2005**, *109*, 7223–7236.
(37) Drobizhev, M.; Stepanenko, Y.; Rebane, A.; Wilson, C. J.; Screen, T. E. O.; Anderson, H. L. *J. Am. Chem. Soc.* **2006**, *128*, 12432–12433.
(38) Screen, T. E. O.; Thorne, J. R. G.; Denning, R. G.; Bucknall, D. G.; Anderson, H. L. *J. Am. Chem. Soc.* **2002**, *124*, 9712–9713.
(39) Hoffmann, M.; Kärnbratt, J.; Chang, M.-H.; Herz, L. M.; Albinsson, B.; Anderson, H. L. *Angew. Chem., Int. Ed.* **2008**, *47*, 4993–4996.
(40) Hoffmann, M.; Wilson, C. J.; Odell, B.; Anderson, H. L. *Angew. Chem., Int. Ed.* **2007**, *46*, 3122–3125.
(41) Taylor, P. N.; Huuskonen, J.; Rumbles, G.; Aplin, R. T.; Williams, E.; Anderson, H. L. *Chem. Commun.* **1998**, 909–910.

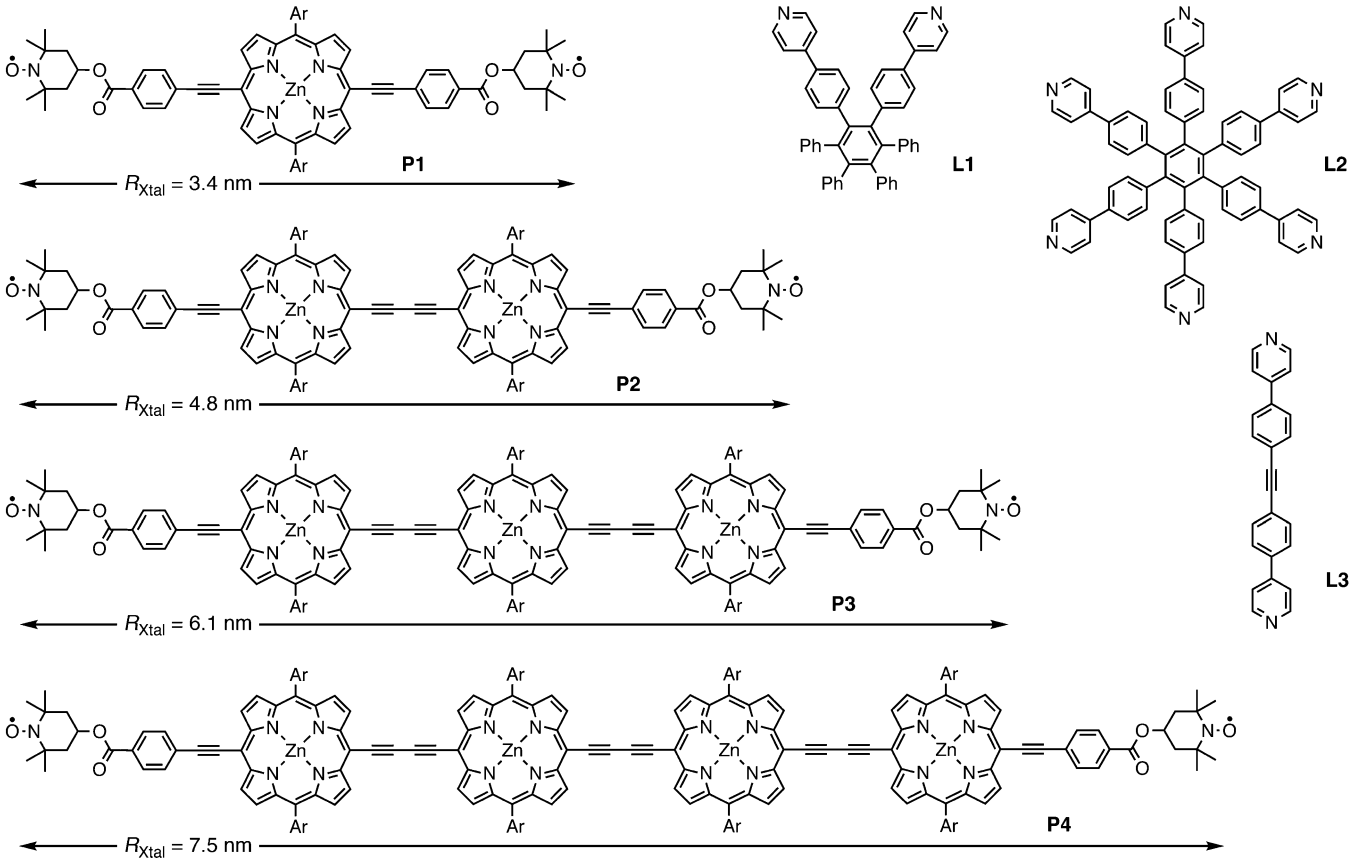

Figure 1. Structures of the TEMPO-terminated porphyrin oligomers **P1**−**P4** and ligands **L1**−**L3** [Ar = 3,5-*bis*(octyloxy)phenyl]. The lengths marked on **P1**−**P4** are the distances between the centers of the N−O bonds in the fully extended molecules (R_{Xtal}), estimated from the crystal structures of **P1′** and a butadiyne-linked porphyrin dimer (Zn−Zn distance: 13.53 Å).[41]

and 1030 data points. The result was averaged by multiple scanning until an acceptable signal-to-noise ratio was acquired, which took between 3 and 24 h.

The data were background corrected using a three-dimensional background function in DeerAnalysis2006.[42] Some DEER time traces needed to be truncated before background correction since pulse overlap was evident (manifested as an artificial upturn in the time trace intensity). The Tikhonov regularization results from DeerAnalysis2006 are shown in the Supporting Information, however the distance distributions from this approach can be poorly determined. A program in Matlab was therefore developed that assumes a predetermined model for the distance distribution, unlike the Tikhonov regularization procedure. The models employed are presented in the relevant Results and Discussion sections. To correct for noise levels in the data, the time traces were normalized to unit intensity at time = 0 by fitting a low-order polynomial to the early part of each curve. Analyzing the data without this correction can lead to results with erroneously short distances. The new program utilizes the pcf2deer function in DeerAnalysis2006 which transforms the predetermined distribution model into a DEER time trace for fitting to the experimental data.[42] Best fits to the DEER time traces were given by those corresponding to the smallest χ^2. The χ^2 is the sum over all points of the squared difference between the experimental and simulated data divided by the error for each point. The error associated with each point in the experiment was the overall linear best fit to the variance between each point and the mean of the 6 surrounding points (±3). The uncertainty in the fitted parameters were estimated from collating all fits that had a χ^2 per degree of freedom value between the value belonging to the best fit and the value plus one. The fits were noticeably poor when the parameters corresponding to the extremes of the uncertainties were used.

Results and Discussion

Synthesis and Crystallography. The TEMPO-terminated porphyrin oligomers **P1**−**P3** were synthesized by Sonogashira coupling of 4-iodobenzoic acid TEMPO ester to alkyne-terminated porphyrin oligomers as shown in Scheme 1. In the case of the tetramer, this route generated byproducts which were difficult to remove, so **P4** was prepared by an alternative route involving Glaser coupling of a mono-TEMPO-terminated porphyrin dimer (see the Supporting Information). Oligomers **P1**−**P4** have flexible side chains [Ar = 3,5-*bis*(octyloxy)phenyl] for high solubility. A TEMPO-terminated porphyrin monomer with *t*-butyl side chains (Ar = 3,5-di-*tert*-butylphenyl), **P1′**, was also synthesized for crystallographic studies. This compound crystallized with two axial dioxane ligands coordinated to the zinc center (Zn−O distances 2.46 and 2.49 Å). The structure is shown in Figure 2. The 6-coordinate zinc atom is in the plane of the porphyrin and the 25-atom porphyrin core is planar (deviation from mean plane: ± 0.125 Å). The meso-aryl substituents are twisted at an angle of 63° to the mean plane of the porphyrin, whereas the conjugated 4-ethynylbenzoate substituents are more nearly coplanar with the porphyrin (torsional angles: 20 and 31°). The TEMPO groups have regular chair geometries, with both oxygen substituents in equatorial posi-

(42) Jeschke, G.; Chechik, V.; Ionita, P.; Godt, A.; Zimmermann, H.; Banham, J.; Timmel, C. R.; Hilger, D.; Jung, H. *Appl. Magn. Reson.* **2006**, *30*, 473–498.

Scheme 1. Synthesis of TEMPO-Labeled Wires[a]

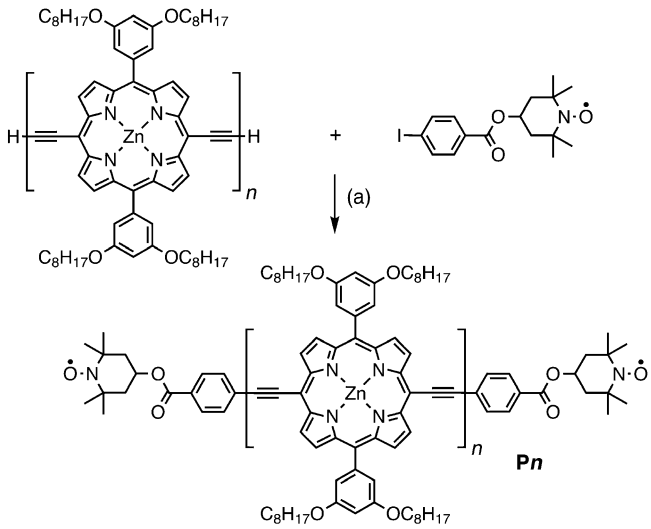

[a] Reagents and conditions: (a) $Pd_2(dba)_3$, CuI, PPh_3, NEt_3, PhMe, 40° C.

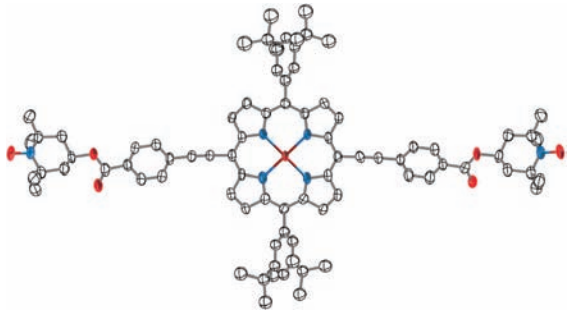

Figure 2. Structure of TEMPO-terminated monomer **P1′** in the crystal (50% probability ellipsoids, omitting hydrogens and coordinated dioxanes for clarity). The intramolecular radical−radical distance, defined as the distance between the centers of the N−O bonds, is 34.36 ± 0.01 Å.

tions. The intramolecular radical−radical distance, defined as the distance between the centers of the N−O bonds, is 34.36 ± 0.01 Å.

Molecular Dynamics Simulations. The spin-to-spin distances, R, in each conformation of each oligomer was measured as the distance between the centers of the N−O bonds. The distance distributions given by binning molecular dynamic (MD) trajectories are shown in Figure 3. These are very well fitted by assuming a semiflexible polymer based on the Kratky−Porod worm-like chain (WLC) model using equations derived by Wilhelm and Frey, which assume a continuously bendable system.[43] The two fitting parameters are the contour length, L, and the persistence length, L_p. The model is based on the statistics for a self-avoiding chain: when $L \ll L_p$, the chain tends toward a rigid rod, whereas when $L \gg L_p$, correlations are lost and the polymer becomes better described as a Gaussian chain.

If κ is L_p/L and r is R/L, when $\kappa\,(1\text{-}r) > 0.2$ the probability density $p(R)$ of the spin-to-spin distance R can be approximated by the two terms in eq 1[42,43]

$$p(R) = \frac{2\kappa}{4\pi}(\pi^2 e^{-\kappa\pi^2(1-r)} - 4\pi^2 e^{-4\kappa\pi^2(1-r)}) \qquad (1)$$

whereas toward the rigid chain limit when $\kappa(1 - r) \leq 0.2$ (i.e., $r \rightarrow 1$), a more complicated expression is required because of the loss of discretization. This is obtained by converting the infinite sum based on eq 1 (which uses the first two terms) to an integral, solving and using the first two terms of the solution to give eq 2.

$$p(R) = \frac{\kappa}{8(\pi\kappa(1-r))^{3/2}}\left[e^{-(4\kappa(1-r))^{-1}}\left(\frac{1}{\kappa(1-r)} - 2\right) + e^{-9(4\kappa(1-r))^{-1}}\left(\frac{9}{\kappa(1-r)} - 2\right)\right] \qquad (2)$$

The WLC model fits to the molecular dynamics results are shown as continuous curves in Figure 3 and the most probable distances from these fits, R_0 (MD) are presented in Table 1.

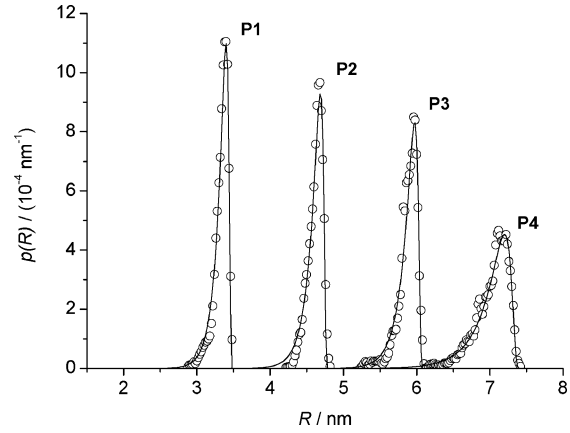

Figure 3. Distance profiles from molecular dynamics simulations (circles) and the WLC fits (see eqs 1 and 2) for each of the wire molecules. $p(R)$ is the probability density that the distance between the centers of the N−O bonds is R.

Table 1. Most-Probable End-to-End Distance (R_0) Results from Fitting the MD Simulations and DEER Experiments with the WLC Model Compared to the Lengths Estimated from Crystal Structures, R_{Xtal} (see Figure 1)

wire	R_{Xtal} (nm)	R_0 (MD) (nm)	R_0 (DEER,d_8-PhMe/Py) (nm)	R_0 (DEER,d_{14}-*o*TP/BnPy) (nm)
P1	3.44	3.40	3.36	3.36
P2	4.79	4.68	4.64	4.60
P3	6.14	5.96	5.88	5.78
P4	7.50	7.20	7.34	7.18

DEER Results for Wires Bound to Monodentate Ligands. The oligomers **P1** to **P4** were measured with DEER in d_8-PhMe/Py and d_{14}-*o*TP/BnPy solvents. All these experiments were carried out at 50 K, but the temperature determining the Boltzmann distribution of conformations is probably the glass-transition temperature of the solvent (120 K for d_8-PhMe/Py and 250 K for d_{14}-*o*TP/BnPy).[44,45] The DEER time traces are shown in Figure 4a (d_{14}-*o*TP/BnPy) and Figure 4c (d_8-PhMe/Py). The shapes of the Pake patterns obtained by Fourier transforming the DEER time traces (see the Supporting Information) do not indicate any exchange coupling; the data appear to result entirely from through-space dipole−dipole coupling.[46−48] The results were fitted with the WLC model described above giving the

(43) Wilhelm, J.; Frey, E. *Phys. Rev. Lett.* **1996**, *77*, 2581–2584.

(44) Murthy, S. S. N.; Gangasharen Nayak, S. K. *J. Chem. Soc., Faraday Trans.* **1993**, *89*, 509–514.

(45) The glass-transition temperatures of *o*TP and toluene are 247.7 and 119.4 K, respectively.[44] DSC experiments showed that the glass-transition temperature of 5% 4-benzyl pyridine in d_{14}-*o*TP is the same as that of pure *o*TP. We assume that the presence of 10% pyridine in toluene has a negligible effect on the glass-transition temperature.

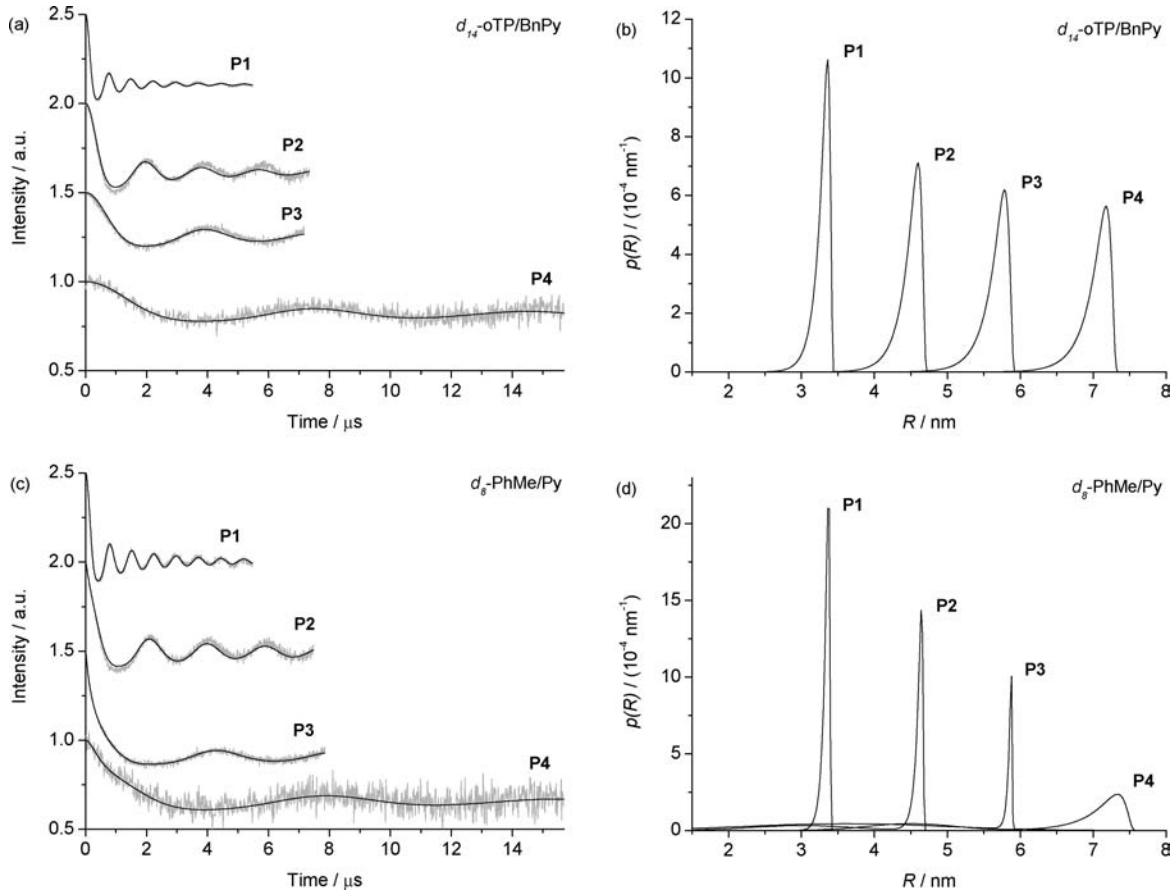

Figure 4. DEER results for the wires **P1**−**P4**: (a) experimental and fitted time traces in d_{14}-*o*TP/BnPy; (b) distance results in d_{14}-*o*TP/BnPy; (c) experimental and fitted time traces in d_8-PhMe/Py; (d) distance results in d_8-PhMe/Py including the Gaussian line shape contributions for **P2**−**P4**.

distance profiles plotted in Figure 4b and Figure 4d. The data for solutions in d_{14}-*o*TP/BnPy fit extremely well to this model, resulting in the modal lengths R_0 listed in Table 1, which agree with the MD simulations. The oligomers dissolved in d_8-PhMe/Py exhibit a component with a fast decay which corresponds to a broad distribution of short distances. We attribute this effect to some disordered aggregation (see the Supporting Information). To fit the WLC model to the data, we included a variable Gaussian line shape to take account of this faster frequency component (the Gaussian parameters were held constant to estimate the uncertainty in the WLC parameters). The modal distance results are summarized in Table 1 and plotted in Figure 5 (for more information including uncertainties, see the Supporting Information). Comparing the DEER data from **P1**−**P4** dissolved in d_{14}-*o*TP/BnPy and d_8-PhMe/Py, it can be seen that the spin-labeled wires are more rigid when frozen in the lower glass-transition temperature d_8-PhMe/Py.[49] For example, contrasting the **P1** time traces in panels a and c in Figure 4 for the two solvent systems shows that the d_8-PhMe/Py sample has less evident damping of the modulations than the wires dissolved in d_{14}-*o*TP/BnPy, which is indicative of a more rigid system.

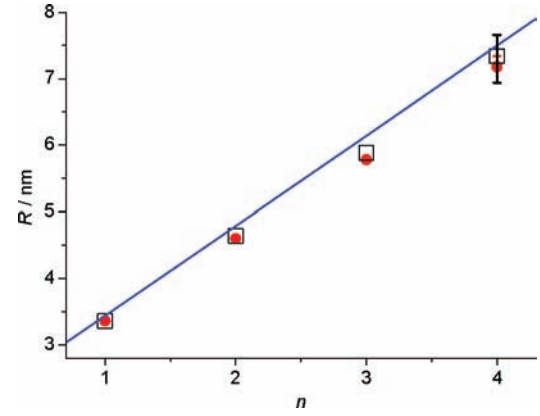

Figure 5. R_0 for the single-strand wires plotted against the number of porphyrin units, *n*, from the DEER results in d_8-PhMe/Py (squares) and d_{14}-*o*TP/BnPy (circles) with fitting uncertainties as error bars (only visible for **P4**). The fully extended radical−radical distances estimated from crystallographic data, R_{Xtal} (see Figure 1) are shown as the blue line, for comparison.

As expected therefore, the end-to-end lengths in the lower temperature d_8-PhMe/Py glass are slightly longer than in d_{14}-*o*TP/BnPy for the longer porphyrin oligomers. The disordered aggregation in the lower temperature glass may also favor the more extended conformation. The radical−radical distances estimated for the fully extended wires from crystallographic data, R_{Xtal} (blue line in Figure 5) are longer than the R_0 values from the MD calculation as expected for these semiflexible systems. The MD R_0 values in turn are slightly longer than the

(46) Weber, A.; Schiemann, O.; Bode, B.; Prisner, T. F. *J. Magn. Reson.* **2002**, *157*, 277–285.
(47) Bode, B. E.; Plackmeyer, J.; Prisner, T. F.; Schiemann, O. *J. Phys. Chem. A* **2008**, *112*, 5064–5073.
(48) Bode, B. E.; Plackmeyer, J.; Bolte, M.; Prisner, T. F.; Schiemann, O. *J. Organomet. Chem.* **2009**, *694*, 1172–1179.
(49) Similar temperature effects were observed on end-labeled oligo(*p*-phenyleneethynylene)s (Prof. G. Jeschke, Physical Chemistry, ETH Zürich, personal communication).

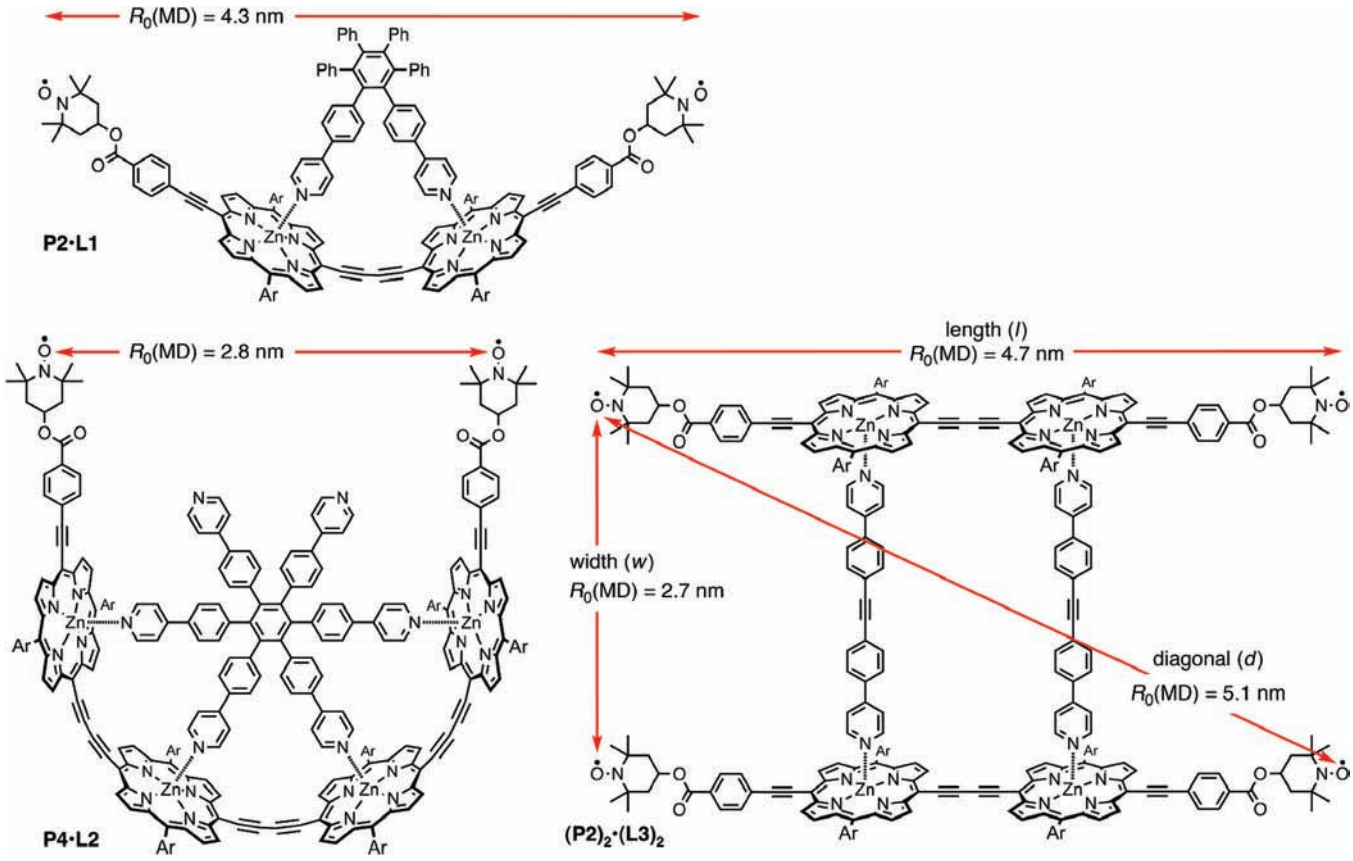

Figure 6. Structures of the Bent Wires, **P2·L1** and **P4·L2**, and the $(\mathbf{P2})_2$·$(\mathbf{L3})_2$ ladder. The most probable distances, R_0, from the MD simulations are shown.

experimental DEER distances for **P1**, **P2**, and **P3**, though closer to those of the oligomers dissolved in d_8-PhMe/Py. The uncertainty in the persistence length fitting parameter, L_p, from the DEER measurements was large, particularly with **P3** and **P4** where the experimental signal-to-noise ratio was worse and fewer modulations were observed. Within a particular data set the values of L_p and L were correlated, with the longest L corresponding to the smallest L_p and vice versa. However, the R_0 (most probable) end-to-end length is a much more stable parameter and so our discussion above is focused on R_0 values. L and L_p fitting results are given in the Supporting Information. Although there is a significant uncertainty in the values of L_p, it is clear that for DEER in both solvents, and also for the MD results, that L_p increases as the chain length increases from **P1**−**P3**. The trend is less evident with **P4** which probably reflects the lower quality of the data for this longest oligomer. This increase in persistence length with increasing chain length indicates that the TEMPO linked end-group is more flexible than the conjugated porphyrin wire backbone. We conclude that a longer porphyrin oligomer of this type would have a persistence length at least as long as that of **P3**, which in d_{14}-*o*TP/BnPy is about 19 nm; in frozen d_8-PhMe/Py the persistence length appears to be substantially longer.

Two previous DEER studies with *bis*-spin-labeled semiflexible conjugated oligomers (poly-*p*-phenyleneethynylenes) modeled the polymer as one or more jointed stiff units, which can bend with respect to each other and are capped at each end by a stiff spin label which can rotate within a defined cone.[19,20] The earlier study showed that the spin label contribution to the flexibility could be successfully removed from the distance distribution using spin label bending, spin label length, backbone stretching, and bending potential as fitted parameters. Jeschke and co-workers also compared their method to the WLC model used in this study and showed that results from the two methods converge as the chain length increased.[19] The second study by Prisner and co-workers exploited the information given by altering the positions of the two microwave frequencies with respect to the nitroxide EPR absorption shape when the nitroxide spin labels have some level of fixed orientation.[20] We have shown that within the bounds of our DEER and MD results, the simple WLC model with two fitting parameters provides adequate information on the flexibility of the wires at two different temperatures.

DEER Results for Wires Bound to Star-Shaped Templates. It has previously been shown that porphyrin oligomers can bend to bind radial template ligands.[35,39,40] Here we show that DEER confirms the bent stuctures of these complexes. We have investigated two complexes: the porphyrin dimer **P2** on the two legged template **L1**, and the porphyrin tetramer **P4** on the six-legged template **L2** (Figure 6).

The WLC model, as applied to the linear wires, is not appropriate for the template-bound molecules because they are not free to move in a random way. Therefore, a Gaussian distribution was assumed for these systems because the distribution should be mainly due to flexibility of the spin label moiety. The Gaussian fitting was implemented in a similar way to above with the mean and full-width at half-maximum (fwhm) of a Gaussian function as fitting parameters.[50]

The DEER data, corresponding distance distributions and calculated MD distributions are shown in Figure 7. At low concentrations (2.7 μM for **P4·L2** and 7 μM for **P2·L1**) in a regime where the UV−vis titration showed clean formation of

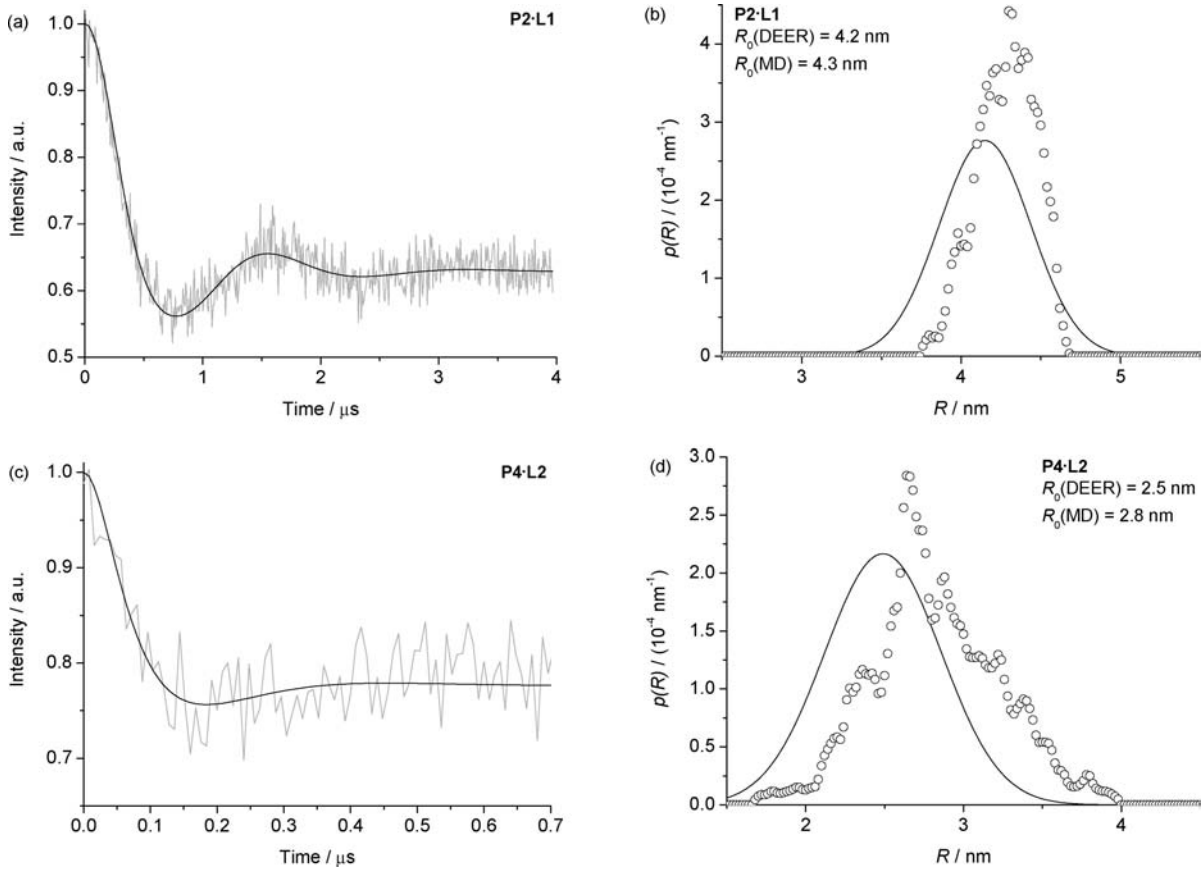

Figure 7. Results for the wires bound to templates in d_8-toluene: (a) **P2·L1** experimental and fitted time trace; (b) MD simulation (circles) and Gaussian distance distribution result from fitting the time trace for **P2·L1**; (c) **P4·L2** experimental and fitted time trace; (d) MD simulation (circles) and Gaussian distance distribution result from fitting the time trace for **P4·L2**.

1:1 complexes (see the Supporting Information), we saw only the distance between nitroxides indicative of the template-bound, rather than unbound, oligomer. We also measured the **P4·L2** at a higher concentration (50 μM) and saw more than the single distance (see the Supporting Information). Therefore, DEER may be a good way of quantifying the degree of template binding since in favorable cases a ratio of template-bound to linear oligomer could be assessed.

For the 1:1 complexes, fitting a Gaussian line shape to the MD simulations for **P2·L1** result gave a mean at 4.30 nm and a fwhm of 0.46 nm. The experimental data were best fitted with a Gaussian centered around 4.15 nm (+0.1/−0.14 nm) and a fwhm of 0.68 nm (+0.47/−0.26 nm). Similarly, the MD simulation for **P4·L2** was fitted with a Gaussian of mean = 2.79 nm, fwhm = 0.94 nm, whereas the experimental data revealed a slightly shorter best distance with mean 2.49 nm (+0.81/−0.35 nm) and fwhm 0.87 nm (+0.86/−0.43 nm). The distance distribution is broader than for the linear wires, reflective of conformational freedom of the TEMPO group around the ester linkage, which will affect the distribution more in the bent structure than in the linear one.

DEER Results for the $(P2)_2\cdot(L3)_2$ Ladder Complex. The porphyrin wire structures discussed in this paper may be used as building blocks for larger arrays.[51] An example of such a structure is analogous to a ladder where the wire forms the side of the "frame" and these are bound by other "rung" molecules (which may be of variable length) via the metal in the porphyrin. Figure 6 shows an example of a ladder system made up from the **P2** wire with dipyridyl rungs **L3**, $(P2)_2\cdot(L3)_2$. These ladder structures have increased hole mobility and two-photon absorption compared to the single-strand wires.[33,37]

Table 2. MD and Fitted DEER Most-Probable (R_0) Distance Results for the $(P2)_2\cdot(L3)_2$ Complex

ladder component	R_0 (MD) (nm)	R_0 (DEER, d_8-PhMe/Py) (nm)
width, *w*	2.69	2.69
length, *l*	4.70	4.62
diagonal, *d*	5.08	4.76

For these systems, there will be three distances corresponding to the inter strand width (*w*, roughly equivalent to the length of the rung joining the two oligomers), which is the shortest distance in this case, wire length (*l*) and diagonal length (*d*), see Figure 6 and Table 2. The distributions of the longer distances (*l* and *d*) from MD calculations fitted well to the WLC model, whereas the shorter distances (*w*) were fitted better by a Gaussian model. The DEER data were modeled using two WLC distributions and one Gaussian distribution; the shapes of these three distributions were fixed from the MD results and their modal distances were adjusted to fit the time traces.[52,53] The fit is shown in Figure 8 and the results are given in Table 2 and the Supporting Information. The χ^2 per degree of freedom error test confirms that the three contributing distances are necessary for a good fit. If the ladder had rectangular (D_{2h}) symmetry, as drawn in Figure 6, then the inter strand distance (w = 2.69 nm) and oligomer length (l = 4.62 nm) would lead to

(50) The full-width at half-maximum (fwhm) corresponds to $2(2\ln 2)^{1/2}\sigma$, where σ is the standard deviation of a Gaussian lineshape.
(51) Taylor, P. N.; Anderson, H. L. *J. Am. Chem. Soc.* **1999**, *121*, 11538–11545.

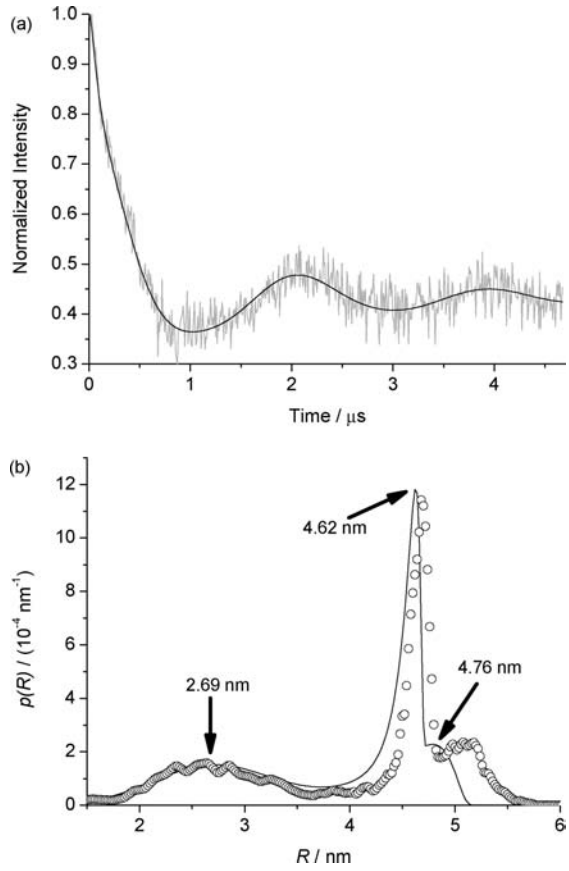

Figure 8. Results for the $(\mathbf{P2})_2\cdot(\mathbf{L3})_2$ ladder in d_8-toluene (30 μM): (a) DEER time trace and fit; (b) MD simulation (circles) and shifted MD components to give best fit to time trace with the resulting R_0 values.

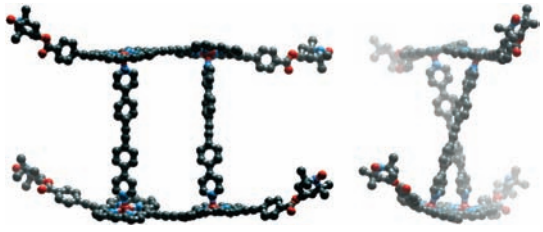

Figure 9. Two orthogonal views of a low-energy conformation of $(\mathbf{P2})_2\cdot(\mathbf{L3})_2$ from the MD simulation, showing a twisted geometry consistent with the DEER data (meso-aryl substituents and hydrogen atoms omitted for clarity).

a diagonal of $d = 5.35$ nm, which is significantly longer than the measured diagonal of 4.76 nm. Thus the results indicate that the structure is twisted in solution, as illustrated in Figure 9. If we assume that the ladder has a regular D_2 geometry, then the twist angle θ can be calculated from the equation $\cos\theta = (l^2 - w^2)/d^2$; application of this equation to the DEER data gives a twist angle of 44°. The wide distance distributions for the width and diagonal length demonstrate that a range of conformations were measured by DEER. Preliminary DEER data were also recorded on a three-rung ladder complex, $(\mathbf{P3})_2\cdot(\mathbf{L3})_3$, giving an experimental distance distribution which is consistent with the result from MD calculations, although the diagonal distance and length could not be resolved, see the Supporting Information.

Conclusions

We have synthesized porphyrin-based molecular wires, **P1**−**P4**, with terminal nitroxide spin-labels in order to assess their conformational flexibility using DEER spectroscopy. The results from these EPR measurements, in two different frozen solvent glasses (with glass-transition temperatures of 120 and 250 K) show that these molecular wires are remarkably rigid. In all cases, the ratio of the experimental modal end-to-end distance R_0 to the corresponding distance in the fully extended conformation, calculated from crystallographic data, R_{Xtal} is in the range $R_0/R_{Xtal} = 0.94-0.98$. A slight increase in rigidity in the lower temperature glass is evident from the less damped DEER time traces, narrower distance distributions, and longer modal lengths recorded in toluene. The distance distributions from these DEER experiments fit well to a wormlike chain model, giving a well-defined modal length R_0. The persistence lengths L_p are poorly determined by the data but the results indicate that for longer oligomer chains of this type, L_p is greater than 19 nm at 250 K. Molecular dynamics calculations (using the MM+ force field at 180 K) gave distance distributions which match well with the DEER results. Previously the conformations of two other types of conjugated oligomers have been investigated by DEER;[18,19] comparison with these previous studies indicates that butadiyne-linked porphyrin oligomers have similar flexibility to poly(*p*-phenyleneethynelene)s.

A special feature of metalloporphyrin-based molecular wires is that their conformations can be controlled by noncovalent self-assembly with multidentate amine ligands. Three supramolecular self-assembled structures, **P2·L1**, **P4·L2**, and $(\mathbf{P2})_2\cdot(\mathbf{L3})_2$ were investigated by DEER. The experimental spin-to-spin distances in these complexes match the predictions from molecular dynamics calculations, demonstrating that DEER is a valuable technique for gaining structural information on nanoscopic self-assembled supramolecular structures. DEER should become a useful addition to the tool-kit for supramolecular chemistry.

Acknowledgment. We thank the EPSRC for funding, the STFC for granting access to the SRS Daresbury, and the EPSRC Mass Spectrometry Service (Swansea) for mass spectra. S.I.P. acknowledges a URF from the Royal Society. J.E.L. was funded jointly by the EPSRC and University College, Oxford. We thank Dr. Jeffrey Harmer for maintaining the EPR spectrometer and Professor Gunnar Jeschke for useful discussions.

Supporting Information Available: Synthetic procedures, characterization data, and expanded DEER and simulation results (PDF and CIF). This material is available free of charge via the Internet at http://pubs.acs.org.

JA905796Z

(52) Recently, Jeschke and co-workers have presented a method for avoiding systematic errors in DEER measurements on systems with multiple radical correlations.[53] Here, we show that the DEER results are consistent with a ladder structure formation. We hope to extend our investigation to incorporate their new methodology in future work.

(53) Jeschke, G.; Sajid, M.; Schulte, M.; Godt, A. *Phys. Chem. Chem. Phys.* **2009**, *11*, 6580–6591.